Asian Journal of Control, Vol. 11, No. 2, pp. 166–174, March 2009
Published online in Wiley InterScience (www.interscience.wiley.com) DOI: 10.1002/asjc.092

IMAGE-BASED HYSTERESIS MODELING AND COMPENSATION FOR AN AFM PIEZO-SCANNER

Yudong Zhang, Yongchun Fang, Xianwei Zhou, and Xiaokun Dong

ABSTRACT

As an important component of Atomic Force Microscopes (AFM), a piezo-scanner exhibits some undesired nonlinear characteristics, among which the inherent hysteresis largely decreases positioning accuracy during scanning and nano-manipulation process. To alleviate this problem, an image-based approach is proposed in this paper to model and then compensate for the hysteresis behavior of the piezo-scanner. Specifically, some scanning images over standard samples are utilized to identify the parameters of the classical Preisach model (CPM) of hysteresis. On the basis of the obtained model, an inversion-based technique is adopted to design a compensator for the hysteresis of the piezo-scanner. The proposed algorithm presents such advantages as low cost and little complexity since no nanoscale position sensor is required to collect identification data. Some scanning and nano-imprinting results are included to demonstrate the performance of the proposed strategy.

Key Words: Atomic Force Microscope (AFM), hysteresis, image, modeling, compensation.

I. INTRODUCTION

In the field of nanotechnology, an atomic force microscope is a fundamental instrument which plays an important role in applications related with nano-imaging, nano-manipulating, and so on [1]. A 3-dimensional piezo-scanner is usually employed in AFM systems to generate fine displacements, including x, y lateral periodic trajectory for scanning process, desired trajectory for nano-manipulation, and z-displacement for constant force control. As an actuator, a piezo-scanner has many advantages, such as high resolution, fast frequency response, and high stiffness. However, a piezo-scanner usually exhibits some undesired nonlinear characteristics, such as hysteresis, structural dynamics, and creep. These drawbacks increase the difficulty of achieving high quality imaging or completing complex nano-manipulation tasks. As a result, the present scanning operation has to be done under comparatively low frequency so that the influence of the structural dynamics can be ignored. However, even for low frequency scanning, the hysteresis behavior brings image distortion during large scale scanning which decreases the accuracy of the measurement.

Recently, many efforts have been devoted to modeling and compensating for the hysteresis of piezo-scanners. According to the modeling mechanism, there are two types of models describing the hysteresis behavior. The first type is called constitutive model such as Jiles-Atherton (JA) model ([2] offers a numerical implementation of JA model) and homogenized energy model [3]. These models are studied from a viewpoint of magnetization, thus they have explicit physical

Manuscript received February 1, 2008; revised September 29, 2008; accepted December 10, 2008.

All the authors are with the Institute of Robotics and Automatic Information System, Nankai University, Tianjin, China (e-mail: yfang@robot.nankai.edu.cn).

This work was supported by Chinese National Natural Science Foundation under grant 60574027 and Program for New Century Excellent Talents in University (No. NCET-06-0210). The authors would like to thank the support from Being Nano-Instruments Ltd. for their heartful help and the reviewers for their constructive comments and suggestions.

meaning. Unfortunately, to obtain such constitutive models, many parameters sensitive to the operation environment need to be identified. Therefore, these models are not frequently employed in practical systems. The latter type is often referred to as phenomenological model [4–9], which is actually a mathematical approximation for the hysteresis nonlinearity. Most of these models, such as the Duhem model [4], the Bouc-Wen model [5] and the frictional model, are in the form of nonlinear differential equations which bring extremely challenging problem for the design of feedback controller. In contrast to these differential models, the classical Preisach model (CPM) [6] in double integral form is the mostly utilized phenomenological model since it can approach to the actual input-output hysteresis relationship infinitely and its inversion can be achieved via an easy manner.

To weaken the hysteresis nonlinearity, both open-loop and closed-loop control methods have been reported to achieve desired performance on the basis of the above models. In [10], a new dc accurate charge amplifier was shown to significantly reduce hysteresis while avoiding voltage drift simultaneously. In [11], a compensator was designed to reduce the hysteresis behavior of piezo-scanners. In [3], based on the analysis for the homogenized energy model, an inverse filter was constructed to attenuate hysteresis and it finally obtained roughly linear input-output behavior for ferroelectric transducers. In [12], the authors used a modified Prandtl-Ishlinskii model to design an inverse controller that compensates for hysteretic actuator characteristics. Inversions of different models were utilized in most of the above compensating strategies. More recently, some advanced control methods have been successfully implemented on the piezo-scanners utilized in AFM systems to enhance their measurement/manipulation performance. In [13], by utilizing the CPM, Wu *et al.* proposed an inversion-based iterative controller to obtain a better performance for AFM systems. In [14], the design and implementation of an H_∞ controller demonstrates substantial improvements in the positioning speed and precision by eliminating the undesirable nonlinear effects of the actuator.

Unfortunately, either to identify the model parameters or implement feedback control, most of the aforementioned methods require a nanoscale position sensor to measure the actual displacement of the piezo-scanner. However, it is usually difficult and costly in practice to equip commercial AFMs with such nanoscale position sensors on the 3-dimensional piezo-scanner tube. Motivated by this fact, some image-based distortion correcting methods have been developed in [15–17], which mainly post-process the obtained image to eliminate the distortion by employing some standard sample data. These image-based strategies involve no expensive nanoscale position sensors, and they are much easier to implement in practice. The purpose of this image-based research is to alleviate the hysteresis behavior of a piezo-scanner, which is different from [18] of eliminating its dynamic effects. Specifically, in this paper, the CPM is chosen to model the hysteresis nonlinearity of an AFM piezo-scanner due to its high accuracy, and an image-based approach is then designed to identify system parameters. Subsequently, based on the inversion of the obtained CPM, a compensator is proposed to attenuate the hysteresis behavior. Compared with the previous image-based methods, this innovative strategy can model the hysteresis behavior accurately and then compensate for it effectively. Therefore, it enhances image quality through improving the positioning accuracy rather post-processing the obtained image. Experimental results demonstrate that the obtained model accurately describes the hysteresis nonlinearity and the compensator improves the performance of the AFM system effectively.

The rest of the paper is organized as follows. Section II gives a detailed description for the innovative image-based hysteresis modeling strategy, including the introduction of CPM and the explanation of the image-based parameter identification method. In Section III, the recursive implementation of CPM model is presented and an inversion-based compensator is constructed to alleviate the hysteresis nonlinearity. Some experimental results of imaging and imprinting are provided in Section IV to illustrate the efficacy of the proposed strategy. Finally, Section V summarizes this paper and gives some plans for future work.

II. IMAGE-BASED HYSTERESIS MODELING

2.1 Classical Preisach Model (CPM)

The Preisach model is widely used to describe various hysteresis phenomena. It can be regarded as the superposition of series of hysteresis operators called hysteron. As depicted in Fig. 1(a), the play-stop operator is often utilized with output as 0 or 1.

Define $u(t) \in \mathbb{R}$, $v(t) = \gamma_{\alpha\beta} \in \mathbb{R}$, $t \in [0, T]$ as the input and output of the hysteron corresponding to a pair of threshold (β, α) with $\beta \leq \alpha$ respectively. Then with an on/off variable $\xi \in \{0, 1\}$, the initial value of

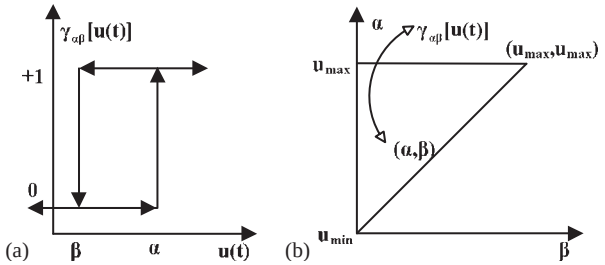

Fig. 1. (a) The play-stop Preisach operator, range {0, 1} with threshold (β, α); (b) the triangle area is the integral region of CPM. CPM is defined as the integral of the weighted Preisach operator over this region.

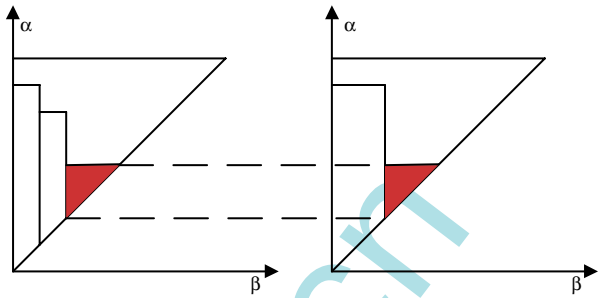

Fig. 2. Congruency property, the integral values of the filled triangle in the two integral planes are equal whereas the previous input may be different.

the hysteresis operator can be described as [7]:

$$v(0)\triangleq\begin{cases}0 & u(0)\le\beta\\ \xi & \beta<u(0)<\alpha\\ 1 & u(0)\ge\alpha\end{cases}\quad(1)$$

Assume that $X_t\triangleq\{\tau\in(0,t]:u(\tau)=\beta \text{ or } \alpha\}$ as the time set when $u(t)$ crosses the threshold β or α, then the output of this operator during $t\in(0,T]$ can be obtained as follows:

$$v(t)\triangleq\begin{cases}v(0) & \text{if } X_t=\emptyset\\ 0 & \text{if } X_t\neq\emptyset \text{ and } u(\max X_t)=\beta\\ 1 & \text{if } X_t\neq\emptyset \text{ and } u(\max X_t)=\alpha\end{cases}\quad(2)$$

The CPM is defined as the double integral over the triangle region (see Fig. 1(b)) in which every point represents a hysteron, and for each hysteron, there exists a corresponding weight $\mu(\alpha,\beta)\in\mathbb{R}$:

$$f^P(t)=H[u(t)]=\iint_{\alpha\ge\beta}\mu(\alpha,\beta)\gamma_{\alpha\beta}[u(t)]d\alpha d\beta\quad(3)$$

where $f^P(t)\in\mathbb{R}$ is the output of the CPM, and $\gamma_{\alpha\beta}[u(t)]\in\mathbb{R}$ stands for the output of the hysteresis operator.

The CPM has numerous properties, among which congruency property is a kernel nature which states that whenever the integral values of the filled triangle in two integral planes are equal, the output of the model corresponding to a minor loop input is independent of the previous input (Fig. 2). This property will be utilized in the subsequently proposed image-based hysteresis modeling method, since when an AFM is employed to scan samples, the input of the piezo-scanner is usually chosen as a periodic triangle signal.

Remark 1. As can be seen from (1) and (2), the value of $\gamma_{\alpha\beta}[u(t)]$ in the CPM not only relies on the current input $u(t)$, but also relates to the previous input. Due to this merit, the CPM can capture the hysteresis characteristic remarkably. Therefore, it is effective for the description of the static hysteresis nonlinearity of AFM piezo-scanners under low scanning frequency.

2.2 Image-based parameters identification

The key issue of modeling hysteresis is to determine the weights of the integral plane. From (3), it can be seen that the twice differentials have to be calculated in order to obtain these weights. This step often leads to large error because of the noise amplification effect of the differential operation. In this research, a discrete recursive method, which is easy to implement in computer, is designed to avoid this problem. That is, compared with conventional modeling process with nanoscale position sensors, an innovative data collection and parameter identification strategy is designed which only requires some image data obtained from the scanning of standard samples. Specifically, based on the congruency property and the periodicity of the input signal, some scanned image data is employed to determine the parameters of the CPM by going through the following four steps.

Step 1. Sample scanning and image collection

The objective of this step is to obtain input-output data of the AFM piezo-scanner for the subsequent parameter identification task. Since no position sensor is available for the measurement of the output displacement, in this research, an indirect way based on sample scanning and image analysis is adopted to calculate the displacement of the piezo-scanner related with specific input. To collect input-output data, the input voltage exerted on the AFM piezo-scanner varies evenly within a pre-defined range. In order to obtain precise estimation of the scanner displacement, standard sample with known period (such as a calibration grating) is scanned

under a comparatively low frequency so that the dynamics of the AFM system can be ignored. Hence, the displacement of the piezo-scanner can be obtained by counting the number of periods in the sample image since the period of the sample is known as a prior.

Remark 2. Creep effects become remarkable for a long time scanning operation. However, for the sample scanning and image collection process involved in this paper, since only one line of the sample is scanned periodically rather than an overall image for each scanning range, the creep effects can be ignored without causing much error.

Step 2. Image data analysis

On the basis of the obtained image, some analysis techniques, such as the center of gravity method, can be applied to extract the feature points, which represent the peak points of the sample. For the sake of simplicity, the following formula can be utilized to set the threshold T:

$$T = \frac{\sum_{i=1}^{n} height(i)}{n} a + c \tag{4}$$

where n is the total number of scanned points, c and a are some parameters adopted to eliminate the effects of the scanning noise which can be set as $a = 1, c = 0$ in the case of little noise, $height(i)$ represents the height information of the ith point. By comparing with the threshold T, we can divide the image into some segments of which some are greater than the threshold T. After that, the coordinates of feature points C_f can be extracted from these segments as follows:

$$C_f = \frac{\sum_{i=C_s}^{C_e} (i * height(i))}{\sum_{i=C_s}^{C_e} height(i)} \tag{5}$$

where C_s, C_e are the starting and ending coordinates of certain segment, with $height(i)$ being the height of sample surface at point i subject to the constraint of $height(i) \geq T$.

Step 3. Polynomial curve fitting

Since the obtained two adjacent feature points represent two neighboring peak points of the sample, their distance is equal to the period of the standard sample, and it should be invariant with different adjacent points if the sample is completely periodic. Based on this fact, the displacements of the piezo-scanner can be obtained by counting the number of the feature points, while the input voltage is directly obtained by multiplying the space voltage with its coordinate. After that, the input-output map is approximated by a polynomial curve through the least square method (LS):

$$\hat{\theta} = (\Phi_N^T \Phi_N)^{-1} \Phi_N^T y_N \tag{6}$$

where $\hat{\theta} \in \mathbb{R}^{m+1}$ is the parameter vector of the polynomial curve with order m, and $\Phi_N \in \mathbb{R}^{N \times (m+1)}$ denotes the input voltage matrix with N being the number of the feature points, and $y_N \in \mathbb{R}^N$ is referred to as the output vector, that is, the displacements of the piezo-scanner corresponding to the feature points.

Step 4. Weights calculation

For each scanning range, the relative displacements of integral curve vertices are computed through a similar polynomial curve approximation. Finally the weights of all blocks in the discrete integral plane can be calculated recursively.

III. INVERSION-BASED COMPENSATION

3.1 Recursive implementation of the CPM

As stated in the previous section, the weights of the discrete integral plane can be obtained based on the scanned image data. After that, a recursive implementation of the CPM is utilized to obtain a continuous inversion of the CPM by adopting the first reversal function (FORF) method [6].

As depicted in Fig. 3(a), f_α stands for the displacement of the piezo-scanner when the input ascends from u_{min} to α, while $f_{\alpha\beta}$ stands for the displacement of the piezo-scanner when the input descends to β after ascending from u_{min} to α. The function f_α and $f_{\alpha\beta}$ are called first order reversal functions. We can easily obtain the values of f_α and $f_{\alpha\beta}$ when α and β are vertices of the integral plane since the weight of each block in the discrete integral plane is already known. For any other values of α and β, the interpolation method is utilized

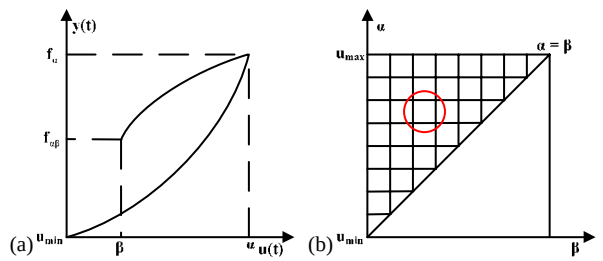

Fig. 3. (a) shows the first order reversal function with (α, β) located in the integral plane; (b) shows an example of the interpolation process. That is, any FORF value can be obtained through the four values of the rectangle vertices which are available from Section II.

to calculate f_α and $f_{\alpha\beta}$:

$$f_{\alpha\beta} = c_0^{\alpha\beta} + c_1^{\alpha\beta}\alpha + c_2^{\alpha\beta}\beta + c_3^{\alpha\beta}\alpha\beta \tag{7}$$

where the coefficients (c_0, c_1, c_2, c_3) is relative to each discretized area. As shown in Fig. 3(b), the coefficients (c_0, c_1, c_2, c_3) corresponding to the rectangle in the circle can be obtained by solving the equation group which is formed by substituting the values of the four vertices into equation (7). Consequently, for any (α, β) located in the rectangle, its FORF value will be available through equation (7).

As the first order reversal functions can be computed by (7) for any α and β, the output corresponding to $u(t_n)$ can be expressed as:

$$f^p(t_n) = f^p(t_m) + f_{u(t_n)} - f_{u(t_n)u(t_m)} \tag{8}$$

where $f^p(t_n)$ is the displacement at t_n, $f^p(t_m)$ is the absolute displacement of the piezo-scanner at the starting voltage.

3.2 Inversion-based compensation of hysteresis

In this section, based on the recursive implementation of the CPM, an inversion of the CPM is constructed to compensate for the hysteresis nonlinearity. As depicted in Fig. 4, the tracking signal $r(t)$, together with the obtained CPM, is utilized to calculate a suitable input $u(t)$ into the piezo-scanner to achieve the desired performance.

Substituting the interpolation equation (7) into (8) yields:

$$\begin{aligned} f^p(t_n) = {} & f^p(t_m) + c_0^{u(t_n)} + c_1^{u(t_n)}u(t_n) + c_2^{u(t_n)}u(t_n) \\ & - (c_0^{u(t_n)u(t_m)} + c_1^{u(t_n)u(t_m)}u(t_n) \\ & + c_2^{u(t_n)u(t_m)}u(t_m) + c_3^{u(t_n)u(t_m)}u(t_n)u(t_m)) \end{aligned} \tag{9}$$

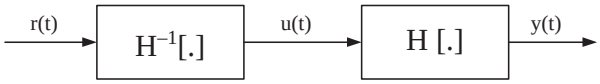

Fig. 4. Compensation framework.

After some mathematical arrangement, (9) can be expressed as:

$$\begin{aligned} f^p(t_n) = {} & f^p(t_m) + c_0^{u(t_n)} - c_0^{u(t_n)u(t_m)} \\ & - c_2^{u(t_n)u(t_m)}u(t_m) \\ & + (c_1^{u(t_n)} + c_2^{u(t_n)} - c_1^{u(t_n)u(t_m)} \\ & - c_3^{u(t_n)u(t_m)}u(t_m))u(t_n) \end{aligned} \tag{10}$$

Then, the desired input voltage can be easily obtained such that:

$$u(t_n) = \frac{f^p(t_n) - f^p(t_m) - c_0^{u(t_n)} + c_0^{u(t_n)u(t_m)} + c_2^{u(t_n)u(t_m)}u(t_m)}{c_1^{u(t_n)} + c_2^{u(t_n)} - c_1^{u(t_n)u(t_m)} - c_3^{u(t_n)u(t_m)}u(t_m)} \tag{11}$$

Now, the remaining problem is to determine these coefficients appeared in (11). The following procedures are adopted to calculate the input after compensation.

(a) Set $u(t_n) = u(t_{n-1})$ to obtain a group of coefficients;
(b) Substitute these coefficients into equation (11). When the acquired $u(t_n)$ and the one set previously in (a) or (c) are in the same block of the integral plane, it implies that these coefficients are valid, and $u(t_n)$ is then the designed input at t_n, as a group of coefficient is corresponding to a discretized block of the integral plane. Hence the process can be stopped; otherwise, these coefficients are still incorrect, in this case, the process starting from step (c) has to be repeated to obtain suitable coefficients.
(c) As the input is monotonically increasing, set $u(t_n) = u(t_n) - \Delta u$, where Δu is the space of the integral region, then go to (b) to update the group of coefficients.

The inversion-based compensation algorithm described above is utilized for the duration when the actuating voltage is ascending. After following the same process, the compensation strategy for descending input can be similarly obtained based on the expressions of (9) and (11). Hence, the triangle trajectory for bidirectional scanning and random trajectory for nanomanipulation can be compensated exactly.

For the desired scanning scope, the compensation work is done as the following steps. Firstly, the input range is computed using recurrence method. Secondly, based on the inverse compensation, an input sequence which amounts to the desired pixels is calculated.

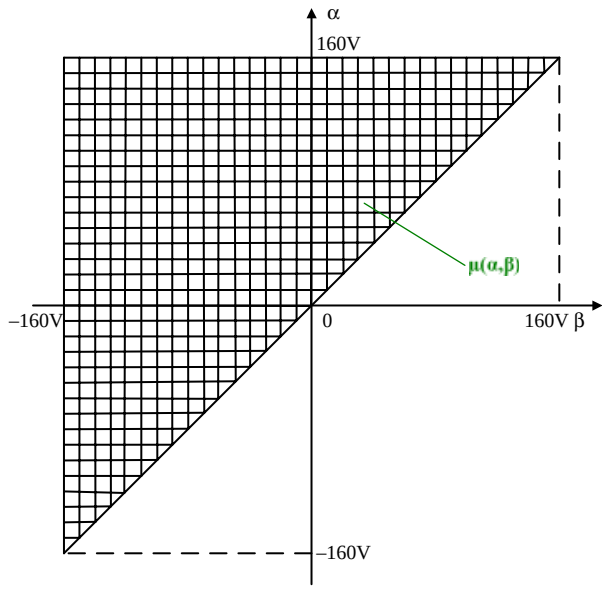

Fig. 5. Discretized integral plane. The input of the piezo-scanner ranges from −160 V to 160 V, and it is divided into 32 sub-ranges with a space of 10 V.

Finally this input sequence is applied to the piezo-scanner to execute the scan process so that a high quality scanning image can be achieved.

Remark 3. As the proposed compensation algorithm successfully addresses the hysteresis of the piezo-scanner for any desired trajectory, the bi-directional scanning mode can be possibly achieved by applying this technology to AFM systems, while most current AFMs offer only one direction scan due to the hysteresis nonlinearity. In general, this research work will not only enhance scanning accuracy, but it is also possible to speed up scanning rate and reduce damage to samples simultaneously. Besides, for any nano-manipulation tasks, the suitable input of the piezo-scanner can be calculated based on the desired trajectory by employing this method.

IV. EXPERIMENTAL RESULTS

To verify the performance of the proposed image-based hysteresis modeling and compensation strategy, the Benyuan CSPM 4000 AFM system produced by Being Nano-Instruments Ltd. is utilized as the experimental testbed. In this AFM system, the probe produced by Mikromasch and piezo-scanner customized by PI are utilized. Based on this testbed, the CPM of the piezo-scanner is obtained and an inversion-based compensator is then constructed to eliminate the hysteresis

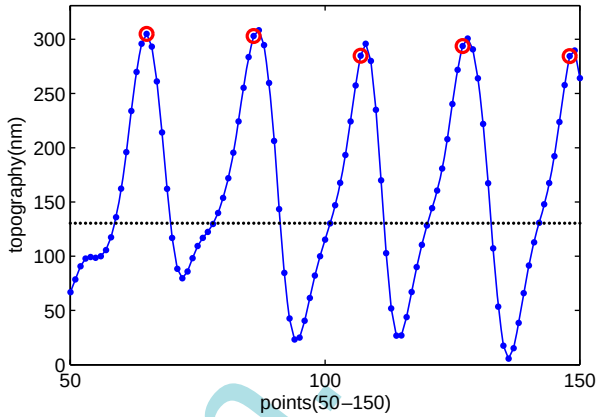

Fig. 6. Feature points obtained via the center of gravity method, where the points circled are the feature points, and the bold line is chosen as the threshold.

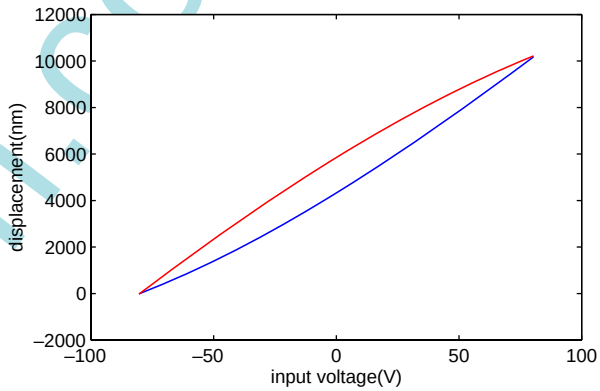

Fig. 7. Approximation curves from least square method.

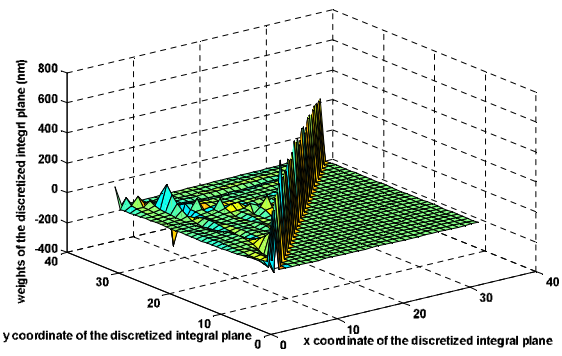

Fig. 8. Three dimensional graphics of weights for the piezo-scanner utilized in the AFM (Benyuan CSPM 4000, P.R. China).

effect of the scanner. After that, both nano-imaging and nano-manipulation tasks are executed upon this AFM instrument to evaluate the efficiency of the proposed image-based modeling and compensation strategy.

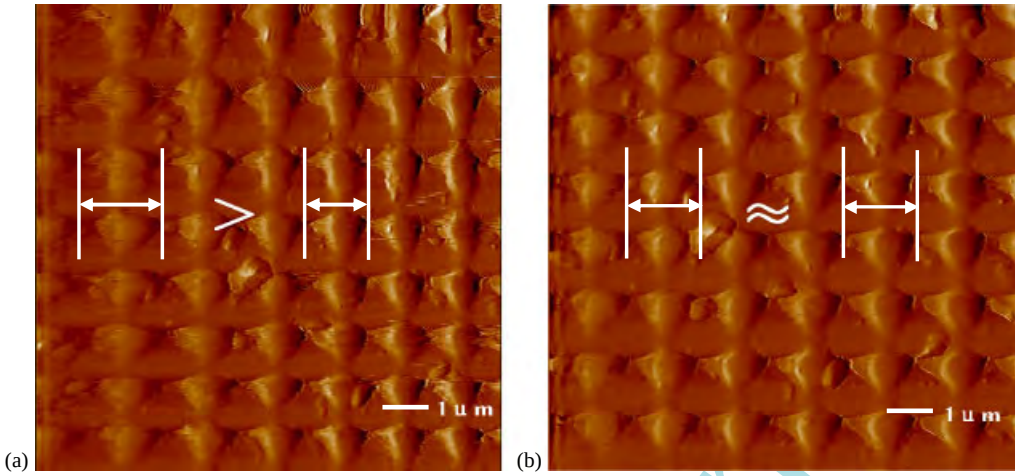

Fig. 9. Scanned topography results of the scanning over a periodic calibration grating: (a) without hysteresis compensation and (b) with compensation for hysteresis.

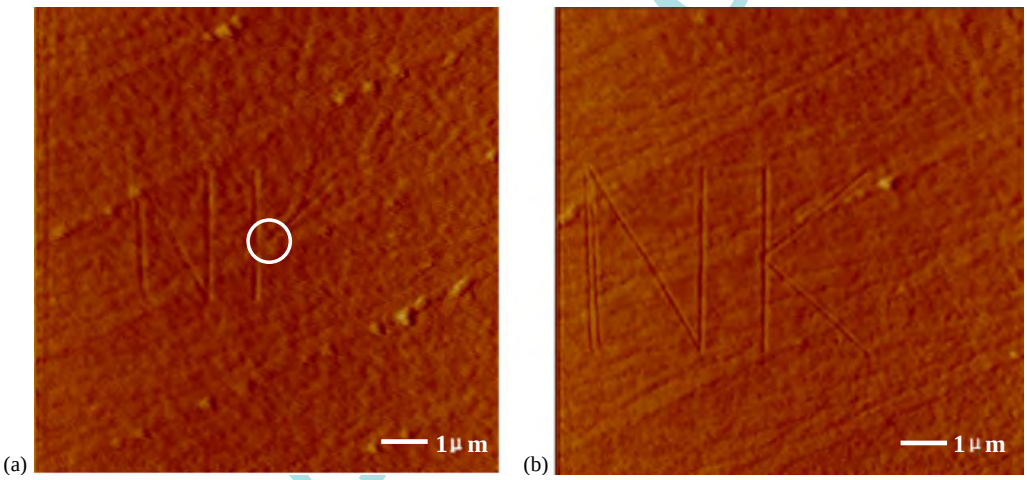

Fig. 10. Imprinting results on polycarbonate: (a) without hysteresis compensation and (b) with compensation for hysteresis.

4.1 Hysteresis modeling and compensator construction

To obtain input-output data of the AFM piezo-scanner, the input voltage exerted on the scanner ranges from -160 V to 160 V, and it is evenly divided into 32 sub-ranges to obtain a discrete integral plane as Fig. 5. A one dimension calibration grating is utilized as the standard sample whose nominal period is 278 nm. The center of gravity method is utilized to extract feature points from the scanning image. As illustrated in Fig. 6, the points marked by the circles are some feature points corresponding to those segments. Based on the obtained feature points, the polynomial curve, and then the weight of each block in the discrete integral plane can be calculated. These results are shown in Fig. 7 and Fig. 8, respectively. After obtaining the CPM model, an inversion-based compensator can be easily constructed by utilizing the strategy stated in Section III.

Remark 4. For the same AFM testbed, as the CPM model obtained by the proposed method gives a good description for the system behavior, the hysteresis modeling and compensator constructing process need not to be done frequently. However, for a long time operation or in the case of very different environment, the calibration work has to be re-done in order to achieve a better compensation for the hysteresis effect.

4.2 Nano-imaging

A calibration grating with a period of 1.667 μm is chosen as the testing sample. The scanning scope and resolution are set as 10 μm and 512×512 respectively.

In z-axis, the classical proportional-integral-derivative (PID) control method is utilized to keep the output constant. Fig. 9 records the scanning results of the sample topography under the scanning frequency of 1 Hz (one line per second). It can be seen that when the hysteresis is not compensated, the scanning image of Fig. 9(a) presents much distortion and the periodic characteristic of the grating can not be observed from the image due to hysteresis (as marked in the image). In contrast, as shown in Fig. 9(b), the inversion-based compensation algorithm effectively attenuates the hysteresis of the piezo-scanner, and the scanned image reflects the actual topography of the grating accurately, as its periodic characteristic is well displaced. Note that in the lateral direction, y-axis of the piezo-scanner exhibits hysteresis nonlinearity as well as x-axis. Therefore, the compensation algorithm has been implemented in these two positioning axes.

4.3 Nano-imprinting

In order to verify the efficacy of the proposed compensation algorithm for random manipulation task, an imprinting experiment is performed on the polycarbonate material. The letters 'NK' are imprinted with and without hysteresis compensation, respectively. During imprinting, a stiff probe with bigger spring constant is employed and the trajectory is designed following the shortest path principle. Fig. 10 shows the experiment results. It can be seen that the size of the result without compensation (see Fig. 10(a)) is much smaller than desired (about half of the full height), and the strokes in the circle are not connected, which will bring serious problems for some nano-manipulation and nano-fabrication tasks. As shown in Fig. 10(b), the imprinting result after hysteresis compensation has proper size and reasonable shape. This lithography experiment suggests that the proposed compensation approach can be extended to other nano-manipulation tasks.

V. CONCLUSION

In summary, this paper proposes an image-based method to model the hysteresis characteristic of the AFM piezo-scanner. Based on the obtained model, a numerical recursive inversion-based compensator is designed to largely eliminate the effect of hysteresis. Experimental results are provided to show that high quality scanning image can be obtained after the compensation of hysteresis. In addition, due to the attenuation of hysteresis, bidirectional scanning can be possibly achieved which will subsequently enhances scanning speed and accuracy of the AFM systems. Moreover, based on the obtained experimental results, it is believed that the compensation work can improve accuracy of nano-imaging and nano-manipulation tasks as well.

As the image data for modeling is acquired under low frequency, feed-forward control based on the inversion of the static Preisach model can only be implemented with slow scanning speed. Therefore, this method mainly improves imaging accuracy under low frequency. Besides, the effect of creep is not strictly considered in this research. Our future work will be aimed on dynamics and the creep phenomenon of AFM piezo-scanners. In addition, some modern control strategies will be employed to address these factors, which will improve scanning and manipulation performance of AFM systems expectably.

REFERENCES

1. Giessibl, F. J. "Advances in atomic force microscope," *Rev. Mod. Phy.*, Vol. 75, pp. 949–983 (2003).
2. Lederer, D., H. Igarashi, A. Kost, and T. Honma, "On the parameter identification and application of the Jiles-Atherton hysteresis model for numerical modeling of measured characteristics," *IEEE Trans. Magn.*, Vol. 35, No. 3, pp. 1211–1214 (1999).
3. Hatch, A. G., R. C. Smith, T. De, and M. V. Salapaka, "Construction and experimental implementation of a model-based inverse filters to attenuate hysteresis in ferroelectric transducers," *IEEE Trans. Control Syst. Technol.*, Vol. 14, No. 6, pp. 1058–1069 (2006).
4. Oh, J. and D. S. Bernstein, "Semilinear Duhem model for rate-independent and rate-dependent hysteresis," *IEEE Trans. Autom. Control*, Vol. 50, No. 5, pp. 631–645 (2005).
5. Ikhouane, F., V. Mañosa, and J. Rodellar, "Dynamic properties of the hysteresis Bouc-Wen model," *Syst. Control Lett.*, Vol. 56, pp. 197–205 (2007).
6. Hu, H. and R. Benmrad, "A discrete-time compensation algorithm for hysteresis in piezoceramic actuators," *Mech. Syst. Signal Proc.*, Vol. 18, No. 1, pp. 169–185 (2004).
7. Visintin, A., *Differential Models of Hysteresis*, Springer, Berlin (1994).
8. Brokate, M. and J. Sprekels, "*Hysteresis and Phase Transitions*," Springer-Verlag, New York (1996).
9. Banks, H. T., A. J. Kurdila, and G. Webb, "Identification of hysteretic control influence operators representing smart actuators part I: formulation," *Math. Prob. Eng.*, Vol. 3, pp. 287–328 (1997).

10. Fleming, A. J. and S. O. Reza Moheimani, "Sensorless vibration suppression and scan compensation for piezoelectric tube nanopositioners," *IEEE Trans. Control Syst. Technol.*, Vol. 14, No. 1, pp. 33–44 (2006).
11. Croft, D., G. Shed, and S. Devasia, "Creep, hysteresis, and vibration compensation for piezoactuators: atomic force microscopy application," *J. Dyn. Syst., Meas. Control*, Vol. 123, No. 1, pp. 35–43 (2001).
12. Janocha, H., D. Pesotski, and K. Kuhnen, "FPGA-based compensator of hysteretic actuator nonlinearities for highly dynamic applications," *IEEE/ASME Trans. Mechatron.*, Vol. 13, No. 1, pp. 112–116 (2008).
13. Wu, Y. and Q. Zou, "Iterative control approach to compensate for both the hysteresis and the dynamics effects of piezo actuators," *IEEE Trans. Control Syst. Technol.*, Vol. 15, No. 5, pp. 936–944 (2007).
14. Salapaka, S., A. Sebastian, J. P. Cleveland, and M. V. Salapaka, "High bandwidth nano-positioner: A robust control approach," *Rev. Sci. Instrum.*, Vol. 73, No. 9, pp. 3232–3241 (2002).
15. Cai, C. Z., X. Y. Chen, Q. Q. Shu, and X. L. Zheng, "Computer correction for distorted STM images," *Rev. Sci. Instrum.*, Vol. 63, No. 12, pp. 5649–5652 (1992).
16. Stoll, E. P. "Correction of geometrical distortions in scanning tunnelling and atomic microscopes caused by piezo hysteresis and nonlinear feedback," *Rev. Sci. Instrum.*, Vol. 65, No. 9, pp. 2864–2869 (1994).
17. Lapshin, R. V., "Automaitc lateral calibration of tunnelling microscope scanners," *Rev. Sci. Instrum.*, Vol. 69, No. 9, pp. 3268–3276 (1998).
18. Clayton, G. M. and S. Devasia, "Image-based compensation of dynamic effects in scanning tunnelling microscopes," *Nanotechnology*, Vol. 16, No. 6, pp. 809–818 (2005).

Yudong Zhang was born in Weifang, Shandong Province, China, in 1984. Presently he is a Ph.D candidate in Control Theory and Control Engineering at Nankai University where he also received his B.S. in Automation in 2006. His research interests include Atomic Force Microscope control system, nonlinear control, and learning control.

Yongchun Fang received the B.S. degree in electrical engineering and the M.S. degree in control theory and application, both from Zhejiang University, China, in 1996 and 1999, respectively, and the Ph.D. degree in electrical engineering from Clemson University, SC, USA in 2002. From 2002 to 2003, he was a Postdoctoral Fellow at the Mechanical and Aerospace Engineering Department, Cornell University. Since 2003, he has been a professor at the Institute of Robotics and Automatic Information System, Nankai University, Tianjin, China. His current research interests include AFM-based nano-manipulation, visual serving and control of underactuated systems including overhead cranes.

Xiaokun Dong was born in Lingbao, Henan province, China, in 1984. He received the B.S. degree in Automation from Tianjin University, China, in 2005, and the M.S. degree in Control Theory and Control Engineering from Nankai University, China, in 2008. Since 2008, He has been a Control Theory and Control Engineering Ph.D. candidate at the Institute of Robotics and Automatic Information System, Nankai University, Tianjin, China, where he currently works on AFM image processing and AFM-based nano-manipulation.

Xianwei Zhou received the B.S. degree in computer science and technology from Hunan University, Changsha, China, in 2004. He is currently working toward the Ph.D. degree at the Institute of Robotics, Nankai University, Tianjin, China. His current research interests include control of Micro/Nano systems, nano-manipulation and control systems.